Incoherent charge hopping and conduction in DNA and long molecular chains

M. Bixon, Joshua Jortner *

School of Chemistry, Tel Aviv University, Tel Aviv 69978, Israel

Abstract

We establish some relations between the kinetics of incoherent, hopping charge transport in bridged large scale chemical systems or in a single-component duplex DNA, and the electrical properties (electric current (j) and conductance (g)) of these systems connected by two electrodes. We considered two distinct voltage distributions across the equienergetic chain (with N bridge elements, and an intersite hopping rate k), which involve the voltage being biased only across the edge bridge elements (case (i)), and the voltage being equally distributed across the bridge (case (ii)). For sufficiently long chains in the low voltage (Φ) domain, we find that $j = (ek/N)G(\kappa_1,\kappa_{-1})(e\Phi/k_BT)$, where $G()$ is a function of charge injection rates $\kappa_1(\kappa_{-1})$ to (from) the electrode. The low field (constant) conductance is $g = 1.6 \times 10^{-19}(k/N)G\,\Omega^{-1}$. At high voltages we established the existence of a maximal, constant, Φ independent current (j_{max}), where $g \to 0$. For case (i) $j_{max} = ek/N$, being determined by the intersite hopping rate and by N^{-1}, as appropriate for diffusional charge transport. For case (ii) $j_{max} = e\kappa_1$, being independent of the chain length, and determined by the rate of charge injection from the electrode. Finally, we applied our kinetic model for the description of incoherent charge transport in and the electronic properties of a donor–acceptor pair connected by two electrodes.
© 2005 Elsevier B.V. All rights reserved.

Keywords: Charge transport; Incoherent hole hopping; Conductance; Molecular wires

1. Introduction

A significant development in the area of nanoelectronics [1–3] pertains to the conduction of a single molecule or a molecular wire connected by metallic leads [3–11]. Nitzan [12] explored the relation between the coherent conduction property of a donor–acceptor (DA) molecular system to the electron transfer rate in this system. He recently considered the relation between bridge assisted electron transfer rate via sequential hopping in a donor–bridge–acceptor (DBA) system and the zero voltage bias molecular conduction within the same supramolecule [13]. In this note we explore the relations between the kinetics of charge migration via incoherent,

thermal hopping between the bridge elements in a large scale chemical bridged system [14,15] or in DNA [16–43], and the electrical properties (current or conduction) of these systems. In a $B_1B_2\ldots B_N$ molecular bridge the $\{B_n\}$ elements can constitute large organic molecules in a large chemical scale system [14,15], or nucleobases within a double strand of DNA, whose electrical properties attracted considerable interest [16–23].

Charge transport in a 'molecular wire', i.e., a linear chain of molecules interconnected by two electrodes [3,6,7,10,11] can be realized for the common case when the Fermi energies of the electrodes fall between the HOMO and LUMO of the constituents, and correspond to two categories: (a) The superexchange limit for $\tau_{super} \ll \tau_{hop}$. When the superexchange transfer time τ_{super} [11], between electrons at the Fermi levels of the two electrodes, is considerably shorter than the $B_j \to B_{j\pm1}$

* Corresponding author.
   E-mail address: jortner@chemsg1.tau.ac.il (J. Jortner).

hopping time τ_{hop}, unistep superexchange mediated by the molecular wire will be exhibited. In this limit an exponential distance dependence of the rate and of the current is exhibited [3,6,7,10,11]. (b) The hopping limit [3,6,7,10,11]. When $\tau_{\text{super}} \gg \tau_{\text{hop}}$, the electron transport is accompanied by dephasing at each $\{B_j\}$ site [3,13,10,11,15,24–29,44] and the transport can be described in terms of a kinetic scheme, with the individual hopping rates being inferred from quantum mechanical information. The 'transition' between superexchange for short chains and thermally induced hopping in long chains was explored [15,29] and applied to molecular wires [11].

Recently, we stressed [24–29] the aspects of energetic control and thermally induced hopping for (hole) charge transfer within the (positively charged) nucleobases in the DNA duplex [24–43]. The resting sites for holes involve guanine (G), higher energy ($\Delta \simeq 0.20$–0.25 eV) mediating states involve adenine (A), while high-energy ($\Delta \cong 0.5$–0.6 eV) involve thymine (T) and cytosine (C). In a structurally disordered DNA (e.g., λ DNA), and in a one-component DNA (e.g., poly G), three major hole transfer and transport mechanisms between guanine pairs separated by a bridge can be distinguished.

(1) Superexchange mediation in structurally disordered DNA. In the duplex

$$G^+ \begin{pmatrix} A \\ C \end{pmatrix}_n \begin{matrix} G \\ T \end{matrix}_n C \tag{1}$$

with short $(A–T)_n$ bridges, i.e., $n < 4$, superexchange mediated $G^+ - G$ transfer occurs and the unistep rate exhibits an exponential distance dependence, $k \propto \exp(-\beta n)$.

(2) Thermally induced hopping (TIH) via an adenine chain in structurally disordered DNA. This mechanism prevails in a long duplex, Eq. (1), with $n > 4$, via the adenine intrastrand or interstrand $\{A_n\}$ chain [27–29,42]. TIH prevails via thermally activated charge transfer from G to A, followed by hopping transport in the $\{A_n\}$ ($n > 4$) chain to the terminal G nucleobase hole trap. As every Watson–Crick pair mediating between two G bases contains A, long $\{A_n\}$ chains provide an effective interstrand/intrastrand route for TIH.

(3) A DNA single component duplex, e.g., poly$\begin{pmatrix} G \\ C \end{pmatrix}_n$ or poly$\begin{pmatrix} A \\ T \end{pmatrix}_n$. From band structure calculations of electronic coupling matrix elements for intra-strand hole transfer between neighboring (G^+G or A^+A) nucleobases, it appears that undoped, neat, single-component DNA constitutes a large gap (~ 3.5 eV), narrow band (~ 0.1 eV), semiconductor [45–51]. Whether charge transport (following charge injection) in a narrow band semiconductor proceeds via hopping or by a coherent, band-type mechanism, is determined by charge scattering processes. On the basis of the Ioffe–Frohlich–Sewell criterion [52] one can infer that incoherent transport prevails when the band width is smaller than the scattering width $\hbar/\tau_{\text{scattering}}$, where $\tau_{\text{scattering}}$ is the relaxation time of the carrier, induced by medium phonons, intramolecular vibrations, and static and dynamic disorder [52]. It was inferred from the wealth of kinetic data for DNA [24–43] that charge transport (at room temperature in DNA) is expected to proceed via hole injection followed by incoherent (strong scattering) hole transfer between adjacent guanine nucleobases.

The mechanisms of charge transport in systems (2) and (3), as well as in large scale $\{B_n\}$ bridged chemical systems, is taken by us to involve incoherent hopping transport via molecular polaron states in vibronic nano-wires [28]. In this paper, we explore the relations between the kinetics of incoherent charge transport and the electrical properties (electrical current and conductance) of these systems connected by metallic leads (electrodes), where charge injection is induced into the edge bridge element. In view of the ubiquity of conflicting experimental data for conductivity of DNA (which were reported to range from properties of an insulator to those of a superconductor) [16–23] a scrutiny of the relevant model systems for DNA ((2) and (3) above) is of interest.

2. Charge hopping kinetics and electric current in DNA and in molecular bridges

We consider charge hopping transport in a molecular bridge which connects two electrodes. The molecular bridge, which may correspond to a large chemical scale system or to a DNA duplex, is composed of $(N + 1)$ constituents $\{B_0\ B_1\ B_2 \ldots B_N\}$. For a DNA duplex of type (2), $B_0 \equiv G$, $B_N = G$ (or GGG), while $B_n = A$ ($n = 1\ldots(N - 1)$). For a DNA duplex of type (3), $B_n = G$ or $B_n = A$ for all n ($= 0 \ldots N$). The LUMO energies of the B_n ($n = 2$ to $(N - 1)$) elements lie above the Fermi level energies E_F of the electrodes, and for any applied voltage these LUMO levels do not come in resonance with E_F. This assumption is valid for low voltages, which will be considered herein. The terminal B_0 and B_N elements of the bridge are strongly (chemically) bound to the electrodes, with charge injection from one electrode (M_1) into the first element (B_0) and an exchange of the charge upon arrival to the last bridge element (B_N) with the second electrode (M_2). Two physical situations for equienergetic chains (e.g., case (3) for DNA) will be considered, which differ by the voltage distribution across the bridge elements.

(A) The voltage is biased only across the terminal bridge elements.
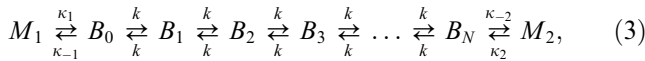(B) The voltage is evenly distributed along the entire bridge.

From a kinetic analysis we shall calculate the steady state charge current (J) for the bridge physical models (A) and (B), which gives the electric current (j) via

$$j = eJ. \tag{2}$$

On the basis of these results we shall be able to infer on the maximal current and the conductance–voltage relations in these nanosystems.

2.1. Steady-state charge transport along the energy equienergetic bridge

We consider steady-state charge hopping transport in an equienergetic chain with the voltage being biased across the first (B_0) and the last (B_N) bridge elements. This system is characterized by the kinetic/electrical scheme

$$M_1 \underset{\kappa_{-1}}{\overset{\kappa_1}{\rightleftarrows}} B_0 \underset{k}{\overset{k}{\rightleftarrows}} B_1 \underset{k}{\overset{k}{\rightleftarrows}} B_2 \underset{k}{\overset{k}{\rightleftarrows}} B_3 \underset{k}{\overset{k}{\rightleftarrows}} \ldots \underset{k}{\overset{k}{\rightleftarrows}} B_N \underset{\kappa_2}{\overset{\kappa_{-2}}{\rightleftarrows}} M_2, \tag{3}$$

k are the forward/backward hopping rates within the bridge. κ_j ($j = \pm 1$ and ± 2) represent charge injection rates to and from the electrodes M_1 and M_2. The charge injection rate from the electrode is assumed to be proportional to the probability that the accepting molecular unit is empty. The overall charge exchange between the metal electrode and the first bridge unit B_0, with an occupation probability A_0, is therefore expressed in terms of the incoming (entering) current

$$J_{\mathrm{in}} = \kappa_1(1 - A_0) - \kappa_{-1}A_0. \tag{4}$$

Similarly, on the other side of the bridge, the charge exchange between the metal and the last bridge unit B_N (with the occupation probability A_N) is given in terms of the outgoing (leaving) current

$$-J_{\mathrm{out}} = \kappa_2(1 - A_N) - \kappa_{-2}A_N. \tag{5}$$

In the present model, we assume that the spatial dependence of an applied voltage bias will be concentrated at the electrode surfaces. Therefore, only the rate constants for the processes between the electrodes and the attached bridge units are influenced by the potential drop. Without a voltage bias the rate constants for charge exchange are identical on the two electrodes, where upon $\kappa_1 = \kappa_2$, $\kappa_{-1} = \kappa_{-2}$. Let the energy difference of an electron between the Fermi surface and the terminal bridge unit be Δ_0. On applying a voltage difference of Φ between the electrodes, one has

$$\kappa_1/\kappa_2 = \exp(e\Phi/k_BT), \tag{6a}$$
$$\kappa_{-2}/\kappa_{-1} = \exp\{(e(\Phi - \Delta_0)/k_BT)\theta(\Phi - \Delta_0)\}, \tag{6b}$$

where $\theta()$ is the step function, i.e., $\theta(x) = 0$ for $x < 0$ and $\theta(x) = 1$ for $x > 0$.

In the steady state situation the charge occupation probabilities $\{A_j\}$ of the $\{B_j\}$ bridge elements are given by

$$dA_j/dt = -2kA_j + k(A_{j-1} + A_{j+1}) = 0, \quad N > j > 0, \tag{7a}$$

while for the edge bridge elements

$$dA_0/dt = \kappa_1 - (k + \kappa_1 + \kappa_{-1})A_0 + kA_1 = 0, \tag{7b}$$
$$dA_N/dt = \kappa_2 - (k + \kappa_2 + \kappa_{-2})A_N + kA_{N-1} = 0. \tag{7c}$$

The steady state charge current J through the bridge is given by

$$J = k(A_j - A_{j+1}). \tag{8}$$

From Eqs. (7) and (8) we infer that the steady state current is proportional to the hopping rate, i.e.,

$$J = k\alpha, \tag{9}$$

which implies that the steady state occupation probability along the bridge is linear, being given by

$$A_j = A_0 - j\alpha. \tag{10}$$

The current conservation for entering and leaving the bridge implies that $J = J_{\mathrm{in}} = J_{\mathrm{out}}$. A straightforward analysis (Appendix A) results in the following expression for the current proportionality constant

$$\alpha = \frac{\kappa_1\kappa_{-2} - \kappa_2\kappa_{-1}}{N(\kappa_{-1} + \kappa_1)(\kappa_2 + \kappa_{-2}) + k(\kappa_1 + \kappa_{-2} + \kappa_2 + \kappa_{-1})}. \tag{11}$$

Eqs. (9) and (11) provide the solution for the steady state current along the equienergetic bridge.

Several limiting cases are of interest. For large values of N, i.e., when $N/k \gg (\kappa_1 + \kappa_{-1} + \kappa_2 + \kappa_{-2})/(\kappa_{-1} + \kappa_1)(\kappa_2 + \kappa_{-2})$, Eqs. (9) and (11) take the form

$$J = (k/N)f(\kappa_1, \kappa_2, \kappa_{-1}, \kappa_{-2}), \tag{12}$$

where

$$f(\kappa_1, \kappa_2, \kappa_{-1}, \kappa_{-2}) = \frac{\kappa_1\kappa_{-2} - \kappa_2\kappa_{-1}}{(\kappa_{-1} + \kappa_1)(\kappa_{-2} + \kappa_2)}. \tag{13}$$

Eqs. (12), (13) and (6) then take the form (assuming that $\kappa_{-2}/\kappa_{-1} \sim 1$)

$$J = (k/N)[\kappa_1\kappa_{-1}/(\kappa_{-1} + \kappa_1)^2][\exp(e\Phi/k_BT) - 1], \tag{14}$$

which for a very low bias, $e\Phi/k_BT \ll 1$, reduces to

$$J = (k/N)[\kappa_1\kappa_{-1}/(\kappa_{-1} + \kappa_1)^2](e\Phi/k_BT). \tag{15}$$

Finally, at a high bias, $e\Phi/k_BT \gg 1$, one expects from Eq. (6) that $\kappa_1 \gg \kappa_2$ and $\kappa_{-2} \gg \kappa_{-1}$. Eqs. (12) and (13) result in

$$J = k/N. \tag{16}$$

At $T = 300$ K, $e\Phi/k_BT = 39\,(\Phi/\text{V})$. The limits of low (high) voltage are realized when $e\Phi/k_BT \ll 1$ ($e\Phi/k_BT \gg 1$), that is $39(\Phi/\text{V}) \ll 1$ ($39(\Phi/\text{V}) \gg 1$). The electrical current, Eq. (2), is given by

$$j = ek\alpha. \tag{17}$$

The electrical properties for the equienergetic chain, with all of the potential drop at the electrode surfaces, Eqs. (11)–(17), are characterized by:

(1) A maximal electric current, j_{max}, for a sufficiently long chain is realized at a high voltage, where j is independent of Φ. According to Eqs. (16) and (17), j_{max} is determined by the hopping rate, $j_{max} \propto k$, and exhibits an "ohmic" type size dependence $j_{max} \propto 1/N$.
(2) The magnitude of the maximal current is $j_{max} = 1.6 \times 10^{-7}\ k/N$ (pA). From our estimates of the hole hopping rates between identical nucleobases in a DNA strand $k \simeq 10^8\ \text{s}^{-1}$ [28,35], we infer that $j_{max} \simeq 16/N$ pA.
(3) The concept of voltage independent conductance g is applicable for the sufficiently low voltage $\Phi \ll 0.026$ V (at $T = 300$ K). The effective conductance $g = \mathrm{d}j/\mathrm{d}\Phi$ assumes the form $g = (e^2/k_BT)(k/N)\kappa_1\kappa_{-1}/(\kappa_1 + \kappa_{-1})^2$. Measurements of j in the sub-pA and pA domain are of interest.

Model calculations (Fig. 1) were performed for the general voltage dependence of the current $j/ek = \alpha$, where α is given by Eq. (11). At a finite voltage we take, according to Eq. (6), $\kappa_1/\kappa_2 = \kappa_{-2}/\kappa_{-1} = \exp(e\Phi/k_BT)$, and we further assume that $\kappa_1 = \kappa_{-2} = \kappa$, whereupon $\kappa_2 = \kappa_{-1} = \kappa\exp(-e\Phi/k_BT)$. Eq. (11) takes the form

$$
\begin{aligned}
\alpha = {}& [1 - \exp(-2e\Phi/k_BT)]/\{N[1 + \exp(-e\Phi)/k_BT]^2 \\
& + 2(k/\kappa)[1 + \exp(-e\Phi/k_BT)]\}.
\end{aligned} \tag{11a}
$$

In the zero voltage limit $\Phi \to 0$, $\alpha = (e\Phi/k_BT)/(2N + k/\kappa)$, which gives the limiting conductance $g = (e^2/k_BT)k/(N + k/\kappa)$. For large voltage $e\Phi/k_BT \gg 1$, we expect the appearance of a maximal current with $j_{max}/ek = (N + k/\kappa)^{-1}$. The relation $j \propto 1/N$, both for the low Φ current and for the maximal current, is realized for $N \gg k/\kappa$. These conclusions are borne out by the model calculations of Figs. 1 and 2, which reveal the linear range of j/ek vs. Φ for low values of $e\Phi/k_BT \sim 39(\phi/\text{V}) \ll 1$, and the saturation of j_{max}/ek towards the value of $(N + k/\kappa)^{-1}$ for large values of $(e\Phi/k_BT) \gtrsim 5$, i.e. $\Phi \gtrsim 0.13$ V. The dependence of the conductance $g = \mathrm{d}j/\mathrm{d}\Phi$ on $e\Phi/k_BT$ (Fig. 1) nicely manifests a constant g value at low Φ values and the vanishing of g at high Φ values. For low values of k/κ (~1), g vs. Φ manifests a monotonous decrease with increasing Φ, while for large values of k/κ (~100) the conductance exhibits a maximum before starting to decrease. This
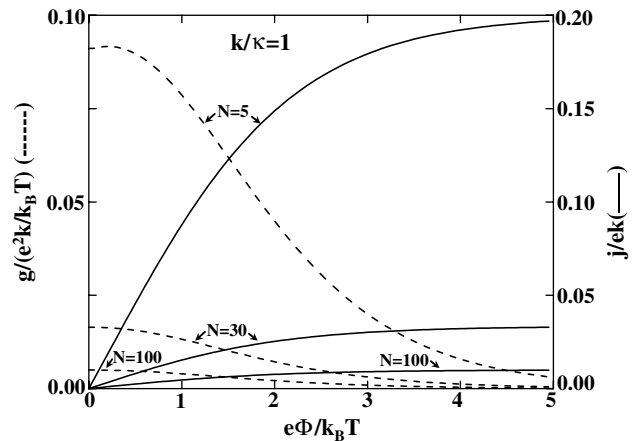

Fig. 1. Model calculations for the voltage (Φ) dependence of the electric current (j) and the conductance (g), for incoherent, hopping charge transport in a $M_1B_0B_1B_2\ldots B_NM_2$ system, where $\{B_n\}$ ($n = 0,\ldots,N$) are the molecular bridge elements thermally connected to the electrodes M_1 and M_2 according to Eqs. (9) and (11). The data are represented in terms of the dependence of j/ek (solid lines, right-side scale) and of $g/(e^2k/k_BT)$ (dashed lines, left-side scale) vs. $e\Phi/k_BT$, where k is the intersite hopping rate, and κ is the charge injection rate. The numbers on the curves represent the chain length N (with the number of molecular constituents being $N+1$). The voltage is biased across the first (B_0) and the last (B_N) bridge elements. Data are for $k/\kappa = 1$ at $T = 300$ K.

maximum is a manifestation of the interplay between charge injection and hopping and does not reflect on an inelastic scattering process.

2.2. Linear voltage bias across the entire bridge

In the foregoing analysis we considered hopping rates which were independent of the electric field, the voltage
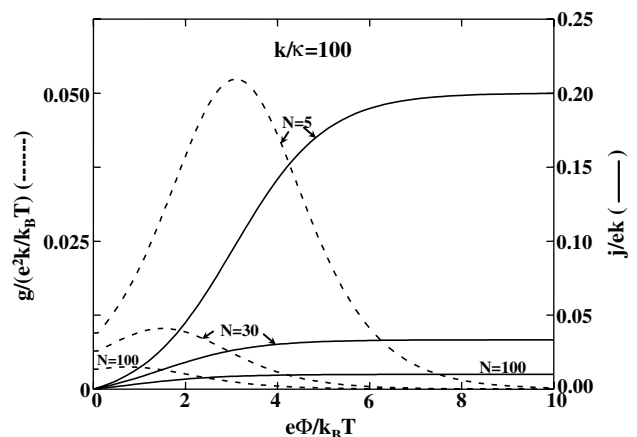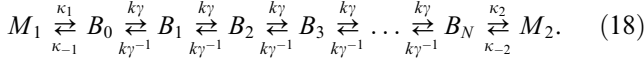

Fig. 2. Model calculations for the voltage dependence of the electric current and the conductance for hopping charge transport in a molecular chain, specified in Fig. 1, with the voltage being biased across the first and the last bridge elements. Data according to Eqs. (9), (11) and (11a) are for $k/\kappa = 100$ at $T = 300$ K, and are represented in terms of j/ek (solid lines, right-side scale) and of $g/(e^2k/k_BT)$ (dashed lines, left-side scale) vs. $e\Phi/k_BT$.

being biased along the terminal bridge elements. We shall now consider the implications of an even electric field bias across the entire bridge. Due to the external field with the voltage Φ (applied between the electrodes), there is a forward bias in the hopping rate constants for charge transfer among the bridge elements in the isoenergetic chain. The kinetic/electrical scheme is

$$M_1 \underset{\kappa_{-1}}{\overset{\kappa_1}{\rightleftarrows}} B_0 \underset{k\gamma^{-1}}{\overset{k\gamma}{\rightleftarrows}} B_1 \underset{k\gamma^{-1}}{\overset{k\gamma}{\rightleftarrows}} B_2 \underset{k\gamma^{-1}}{\overset{k\gamma}{\rightleftarrows}} B_3 \underset{k\gamma^{-1}}{\overset{k\gamma}{\rightleftarrows}} \ldots \underset{k\gamma^{-1}}{\overset{k\gamma}{\rightleftarrows}} B_N \underset{\kappa_{-2}}{\overset{\kappa_2}{\rightleftarrows}} M_2. \quad (18)$$

The forward hopping rate is $k\gamma$, while the backward hopping rate is $k\gamma^{-1}$, where the rate constant k corresponds to the hopping rate in the unbiased case. The forward bias is given by γ^2, where

$$\gamma^2 = \exp(\Delta\varepsilon/k_B T) \quad (19)$$

and the nearest-neighbor (voltage induced) energy gaps are

$$\Delta\varepsilon = E(B_{j-1}) - E(B_j) = e\Phi/N, \quad (20)$$

so that

$$\gamma = \exp(e\Phi/2Nk_B T). \quad (21)$$

The kinetic system of equations for the population probabilities in the steady state is

$$\frac{dA_j}{dt} = -k(\gamma^{-1} + \gamma)A_j + k(\gamma A_{j-1} + \gamma^{-1}A_{j+1}) = 0, \quad (22)$$

$$\frac{dA_0}{dt} = \kappa_1 - (k\gamma + \kappa_1 + \kappa_{-1})A_0 + k\gamma^{-1}A_1 = 0 \quad (23)$$

$$\frac{dA_N}{dt} = \kappa_2 - (k\gamma^{-1} + \kappa_2 + \kappa_{-2})A_N + k\gamma A_{N-1} = 0. \quad (24)$$

The steady state current, inside the bridge, should obey the relation

$$J = k\gamma A_j - k\gamma^{-1}A_{j+1}. \quad (25)$$

A kinetic analysis (Appendix B) results in the explicit expression for the charge current

$$J = k\left[\frac{\kappa_1\gamma^{2N}(\kappa_2 + \kappa_{-2})}{(\kappa_1 + \kappa_{-1})} - \gamma^{-1}\kappa_2\right]$$

$$\times \left[(\gamma^{-1}k + \kappa_2 + \kappa_{-2}) + \gamma^2(\kappa_2 + \kappa_{-2})\frac{1 - \gamma^{2(N-1)}}{1 - \gamma^2}\right.$$

$$\left. + k\gamma^{2N}\frac{(\kappa_2 + \kappa_{-2})}{(\kappa_1 + \kappa_{-1})}\right]^{-1}. \quad (26)$$

Provided that $(\kappa_1 + \kappa_{-1}) = (\kappa_2 + \kappa_{-2})$, Eq. (26) reduces to

$$J = k(\kappa_1\gamma^{2N} - \gamma^{-1}\kappa_2)$$

$$\otimes \left[(\gamma^{-1}k + \kappa_2 + \kappa_{-2}) + \gamma^2(\kappa_2 + \kappa_{-2})\frac{1 - \gamma^{2(N-1)}}{1 - \gamma^2} + k\gamma^{2N}\right]^{-1}. \quad (27)$$

Taking $\kappa_1 = \kappa_2$, $\kappa_{-1} = \kappa_{-2}$ and defining $\beta = (\kappa_2 + \kappa_{-2})/k$, we can rewrite Eq. (27) in the form

$$J = \kappa_1[\gamma^{2N} - \gamma^{-1}]\left[(\gamma^{-1} + \beta) + \gamma^2\beta\frac{\gamma^{2(N-1)}}{\gamma^2 - 1} + \gamma^{2N}\right]^{-1}. \quad (28)$$

The electrical current is obtained from Eqs. (2) and (28) in the form

$$j = e\kappa_1[\gamma^{2N} - \gamma^{-1}]\left[(\gamma^{-1} + \beta) + \gamma^2\beta\frac{\gamma^{2(N-1)}}{\gamma^2 - 1} + \gamma^{2N}\right]^{-1}. \quad (29)$$

Note that Eqs. (28) and (29) differ only by a factor of e.

In the limit of long chains ($N \gg 1$), when $e\Phi/2Nk_B T \ll 1$ (i.e., $\Phi \ll (2N/39)$ V), Eq. (29) takes the form

$$j = (ek/N)[\kappa_1/(\kappa_1 + \kappa_{-1})][\exp(e\Phi/k_B T) - 1]. \quad (30)$$

Furthermore, at a low voltage, when $\exp(e\Phi/k_B T) - 1 \ll 1$, Eq. (30) is reduced to the form

$$j = (ek/N)[\kappa_1/(\kappa_1 + \kappa_{-1})]e\Phi/k_B T. \quad (31)$$

For the opposite limit of a very high bias of $\gamma \gg 1$ (and $\kappa_1 > \kappa_{-1}$), Eq. (29) gives the limiting value

$$j_{\max} = e\kappa_1. \quad (32)$$

From this analysis we infer that at the low voltage limit, Eq. (31), the conductivity is $g = (e^2/k_B T)(k/N)\kappa_1(\kappa_1 + \kappa_{-1})^{-1}$. For the high voltage bias across the entire bridge, the maximal current, Eq. (32), is determined by the charge injection rate κ_1 from the electrode. Unlike in the cases of field bias on the terminal bridge elements, when the maximal current is realized for $e\Phi/k_B T > 1$ (Section 2.1), in the present case the maximal current is realized for sufficiently high voltages, i.e., $39(\Phi/\text{V})/N \geqslant 1$ (at $T = 300$ K). The maximal electrical current exhibits the $j_{\max} \propto e\kappa_1$ relation and is independent of N. A numerical estimate for the maximal current in such a chain results in $j_{\max} \simeq 1.6 \times 10^{-7}$ (κ_1/s^{-1})pA. The maximal current is independent of Φ, so in this limit $g = 0$.

The general voltage dependence of the current, as obtained from Eq. (29), is displayed, together with the conductance in Figs. 3 and 4 for different values of N and of $\beta = (\kappa_1 + \kappa_{-1})/k$. The dependence of $j/e\kappa_1$ vs. $e\Phi/k_B T$ reveals a linear range of $j/e\kappa_1$ and a constant g for low values of $e\Phi/k_B T \ll 1$, with the initial value of g decreasing with increasing N. The voltage dependence of $j/e\kappa_1$ saturates and the conductivity vanishes for large values of $e\Phi/2Nk_B T$. The conductance exhibits a monotonous decrease with increasing $e\Phi/k_B T$ for lower values of β (~ 0.1–1). With increasing β (towards ~ 10) a maximum in g vs. Φ is exhibited, which may be due to the dominance of the charge injection from the electrodes relative to charge hopping within the chain.
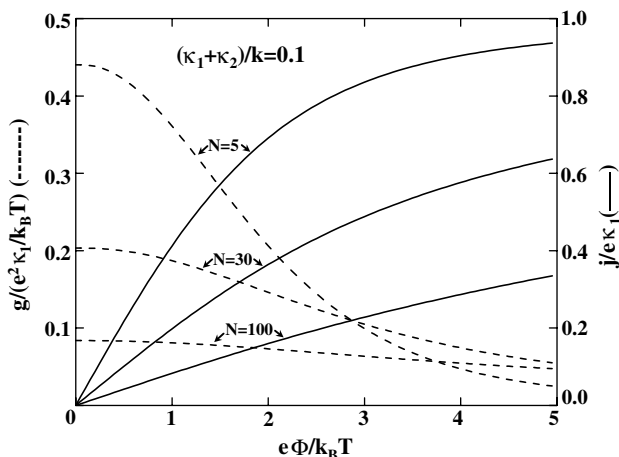
Fig. 3. Model calculations for the voltage dependence of the electric current and the conductance for hopping charge transport in a molecular chain, specified in Fig. 1, with a linear voltage bias across the entire bridge. Data, according to Eq. (29), are for $\beta = (\kappa_1 + \kappa_2)/k = 0.1$ and $T = 300$ K, and are represented in terms of $j/e\kappa_1$ (solid lines, right-side scale) and of $g/(e^2\kappa_1/k_B T)$ (dashed lines, left-side scale) vs. $e\Phi/k_B T$.
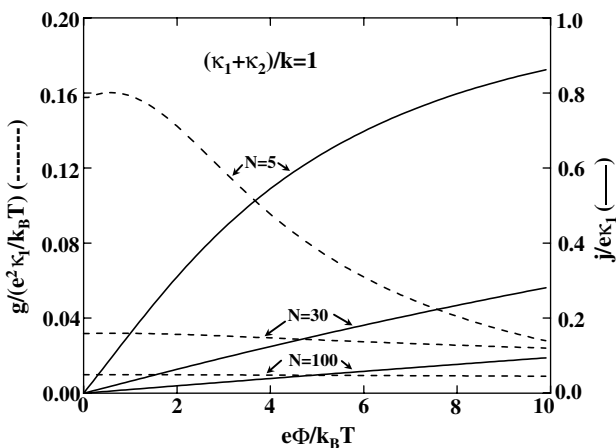

Fig. 4. Model calculations for the voltage dependence of the electric current and the conductance for hopping charge transport in a molecular chain, specified in Fig. 1, with a linear voltage bias across the entire bridge. Data, according to Eq. (29) are for $\beta = (\kappa_1 + \kappa_2)/k = 1$ and $T = 300$ K, being represented in terms of $j/e\kappa_1$ (solid lines, right-side scale) and of $g/(e^2\kappa_1/k_B T)$ (dashed lines, left-side scale) vs. $e\Phi/k_B T$.

3. Concluding remarks

Our analysis provides the relations between incoherent electron transport kinetics and electric properties of several types of large-sized chemical systems and of DNA. The evaluation of electrical current in the molecular chain connected by electrodes led to several results for the maximal current in different model systems. Three major results emerge from our analysis: the concept of a maximal current, the features of the low voltage domain, and the possibility of defining the conductance of the molecular bridge.

(1) The maximal current. For sufficiently high voltages, i.e., $e\Phi/k_B T > 1$ in the isoenergetic chain with the voltage biased only across the edge bridge elements, and $e\Phi/2Nk_B T > 1$ for voltage biased across the entire bridge the current reaches a constant value, which is independent of the voltage. For the isoenergetic chain, with potential bias across the terminal bridge elements, $j_{max} = ek/N$, Eq. (16), is determined by the inter-element hopping rate k, while for the voltage biased hopping, $j_{max} = e\kappa_1$ is determined by the rate of charge injection from the electrode. In the limit of high voltage there are qualitative differences between the models. In the first model the charge motion along the bridge is diffusive. The maximum current can be deduced from the diffusion equation towards a sink with the extreme boundary conditions of a concentration of unity on one side and zero on the other side. The concentration profile is linear and the limiting current is $j_{max} = ek/N$, being independent of the kinetics of charge injection. On the other hand, if the potential changes continuously along the bridge, the rate of charge transport in the bridge increases (effectively) without a bound. As a result the maximum current depends only on the rate of injection.

(2) The low voltage domain. At low potential differences and long bridges, the two models show similar behavior as a function of bridge length and potential difference. In the first model, where all the potential drop appears at the electrode surfaces, the current is given by Eqs. (15) and (17). In the second model, where the potential changes linearly along the bridge, the steady state current is given by Eq. (31). In both cases $j \propto (k/N)\Phi$, with the low Φ conductance being $g \propto (k/N)G(\kappa_1, \kappa_{-1})$. The function $G(\cdot)$ of the charge injection rates from/to the electrodes is different in the two cases.

(3) The electrical conductance of molecular bridges. Among the molecular models explored by us, the constant conductance for low Φ is $g = (e^2/k_B T)(k/N)G(\kappa_1, \kappa_{-1})$ for both cases. At high voltage $g \to 0$ both for the voltage bias across the terminal bridge elements only and for the voltage biased hopping. In some cases a maximum of g vs. Φ is manifested, reflecting on competition between charge injection and intrachain charge hopping.

Some order of magnitude estimates of currents in the incoherent transport domain are in order. The maximal current for the voltage biased isoenergetic chain is $j_{max} = ek/N$, which for a single component DNA was estimated as $j_{max} = 16/N$ pA. Such currents in the pA range are amenable for experimental observation in a single component DNA duplex. The low field conductance assumes the value $g = 1.6 \times 10^{-19}(k/N)G\,\Omega^{-1}$.

Using the estimate for a single-component DNA with $k \sim 10^8 \, \text{s}^{-1}$ [28], the molecular bridge conductance is $g \simeq 1.6 \times 10^{-9}/N \, \Omega^{-1}$. On the other hand, for a linear potential change across the bridge, the low voltage resistance is again expected to show the conductance $g \simeq 1.6 \times 10^{-9}/N \, \Omega^{-1}$, while the high voltage current $j_{\text{max}} = e\kappa_1$ is independent of N and determined by charge injection kinetics. The experimental observation of picoamper currents and $G\,\Omega$ resistance in these DNA nanoelectronic current measurements under appropriate experimental conditions is expected to be realized for proper voltage bias. Prior to the confrontation of the results of the present model calculations for the hopping charge conductivity with experimental reality, several extensions of the theory are required. First, one should provide a detailed treatment of the electrode charge injection kinetics, which was phenomenologically represented in terms of the rates κ_j ($j = \pm 1$, $j = \pm 2$). Second, the inclusion of the effects of inelastic processes, involving vibrational excitation of the molecular components, which were not considered by us, should be incorporated in the treatment of the electrical properties. The available conflicting experimental data [16–23] require further scrutiny. Some reports of metallic [16] and superconducting [20] DNA lack experimental basis [21–23] and theoretical foundation [17,28], while some of the recent experimental data [18–22] support the notion [17,28] that neat undoped DNA corresponds to a large gap, narrow band semiconductor [18] or insulator [17,19–23]. Further experimental studies of charge injection and electrical transport in DNA are called for.

The present study establishes the relation between the electrical properties and the kinetics of incoherent charge transport in large scale molecular systems and in DNA. This relation pertains to incoherent kinetics of charge transport, which is characterized by the sequential hopping events between adjacent sites in the molecular chain (or DNA). Complete erosion of coherence prevails, as the system looses its phase memory at each site, and the population probability is described in terms of the diagonal matrix element of the density matrix. Another limit pertains to coherent transport across the molecular chain, where the mean free path exceeds, or is comparable to, the intersite spacing. The distinction between the incoherent transport limit ($2V < \hbar/\tau_{\text{scattering}}$ [52]) and the coherent transport limit ($2V > \hbar/\tau_{\text{scattering}}$ [52]) in the valence or conduction band large gap semiconductors (with a band width $2V \sim 0.1–1.0$ eV), e.g., DNA, where $2V \simeq 0.1$ eV [24–43] or organic polymers (where $2V \simeq 0.1–1.0$ eV) [14,15,53,54], is governed by the Ioffe–Frohlich–Sewell criterion [52] for the relaxation time ($\tau_{\text{scattering}}$) of the carrier in the band. Several independent guidelines for the identification of the incoherent transfer limit rest on kinetic information:

(1) Kinetic rates for charge injection and transfer. The interpretation of the kinetic data in terms of the traditional charge transfer theory [55], expressing the rate in terms of the product of the square of the electronic coupling and the nuclear Franck–Condon factor, points towards chemically incoherent charge hopping within the bound identical system.

(2) The 'transition' from superexchange unistep charge transfer through short chains of bridge constituents to thermally induced hopping (TIH) in long chains of bridge elements, which are connected to a donor and an acceptor on both sides [11,14,15,28,29,44]. The signature of TIH is manifested by the onset of the weak bridge length dependence on the bridge mediated donor–acceptor charge transfer. A quantitative kinetic analysis of the donor–acceptor charge transfer rates or yields in terms of a charge hopping between the bridge constituents [14,15, 28,29] supports the picture of incoherent charge transport in such a system.

The kinetic data for charge injection [30–39], transfer [30,31,36], transport [24,25,30,31,39] and TIH [28,29,40–43] in double strand DNA segments in solution support the picture of hole injection followed by incoherent hole transport between adjacent identical nucleobases (e.g., (Adenine)$_n$ chains [32,33,41–43]). On the basis of these kinetic data we infer that charge conduction in one-component DNA duplexes like poly(G–C) (with hole transport through the guanines) or poly(A–T) (with hole transport through the adenines) will correspond to the hopping, incoherent transport limit in a system characterized by a narrow bandwidth ($2V \simeq 0.1–0.2$ eV [50,51]). The same situation is expected to prevail in organic oligomer polymers [14,15] which manifest the superexchange – TIH transition [15]. In the incoherent hopping transport limit the charge mobilities are expected to be low, i.e., $\mu \sim 10^{-5}–10^{-3} \, \text{cm}^2/\text{V s}$ [52]. On the other hand, in the coherent band transport limit the charge mobilities are expected to be high, i.e., $\mu = 0.1–1.0 \, \text{cm}^2/\text{V s}$ [52,57]. Such high electron and hole mobilities are manifested in poly-phenylene-vinylene polymers [53,54], indicating that charge transport in these organic semiconducting polymers (with a bandwidth in the region $2V \simeq 0.1–1.0$ eV depending on the torsion angle [56]) corresponds to the coherent transport limit [52,57].

Finally, we address the issue of incoherent charge transport in a single donor (D) – acceptor (A) pair. A theoretical model for the conductance of a D–A pair involving coherent transport was presented by Nitzan [13]. In what follows we advance our kinetic model to describe incoherent charge transport in a DA pair connected by two electrodes (M_1 and M_2), described by the kinetic scheme

$$M_1 \underset{\kappa_{-1}}{\overset{\kappa_1}{\rightleftarrows}} D \underset{k_-^{CT}}{\overset{k^{CT}}{\rightleftarrows}} A \underset{\kappa_2}{\overset{\kappa_{-2}}{\rightleftarrows}} M_2. \tag{33}$$

The forward (k^{CT}) and backward (k_-^{CT}) unistep charge transfer rates (which are taken to be Φ independent, neglecting Stark effects) are well known from electron transfer theory. The charge injection rates are κ_1 (κ_2) from the electrodes to D (A), while the charge injection rates from D (A) to the electrodes are κ_{-1} (κ_{-2}). From the analysis of Appendix C we imply that for a finite, small, voltage drop, the steady state current is

$$j = \frac{ek^{CT}\kappa_1\delta}{\kappa_1\delta + \kappa_{-1}} - \frac{ek_-^{CT}\kappa_2}{\kappa_2 + \kappa_{-2}}, \tag{34}$$

where $\delta = \exp(e\Phi/k_B T)$. Making use of Eq. (C.7), the electric current is

$$j = [ek^{CT}\kappa_1\kappa_{-1}/(\kappa_1\delta + \kappa_{-1})(\kappa_1 + \kappa_{-1})](\delta - 1). \tag{35}$$

In the limit $\kappa_1 \ll \kappa_{-1}$ (which is realized when the direct charge transfer dominates, i.e., $k^{CT} \gg k_-^{CT}$), Eq. (35) results in the simple relation

$$j = ek^{CT}(\kappa_1/\kappa_{-1})[\exp(e\Phi/k_B T) - 1], \tag{36}$$

which, for sufficiently low voltage, reduces to

$$j = ek^{CT}(\kappa_1/\kappa_{-1})(e^2\Phi/k_B T), \tag{37}$$

with the current $j \propto ek^{CT}(\kappa_1/\kappa_{-1})\Phi$ and the constant (Φ independent) conductance being $g \propto k^{CT}$. This result, derived for incoherent DA charge transfer, exhibits an identical dependence of the conductance on the (forward) charge transfer rate, as previously derived for the coherent case [12]. Accordingly, as long as the DA charge transfer is dominated by the forward process, one cannot readily distinguish between the coherent and the incoherent case on the basis of the linear dependence of g on k^{CT}. For the coherent case [12] $g \propto k^{CT}/(FC) \propto V^2$, where (FC) is the nuclear Franck–Condon factor and V is the non-adiabatic electronic D–A coupling. On the other hand, for incoherent transport studied herein $g \propto V^2(FC)$, where (solvent and intramolecular) nuclear distortions contribute to the electrical properties of a single molecule. In the foregoing discussion of the electrical properties of a single DA molecule or of a molecular chain embedded between two electrodes, the Stark effect on the unistep charge transfer rates on intersite hopping rates (in the high fields of 10^7–10^8 V cm^{-1}) was not considered and requires further scrutiny.

Acknowledgements

Appendix A. Steady state current in energy equidistant bridge

The same steady state current, $J = k\alpha$, Eq. (9), should enter and leave the bridge. The leaving current from the terminal unit N is given by

$$J = (\kappa_{-2} + \kappa_2)A_N - \kappa_2 = k\alpha \tag{A.1}$$

from which we can deduce an expression for the occupation of the terminal

$$A_N = \frac{\kappa_2 + k\alpha}{\kappa_2 + \kappa_{-2}}. \tag{A.2}$$

Using Eq. (9), $A_N = A_0 - N\alpha$, which, together with Eq. (A.2), results in the following expression for A_0,

$$A_0 = \frac{\kappa_2 + k\alpha}{\kappa_2 + \kappa_{-2}}. \tag{A.3}$$

Next, we utilize the equations for the current injection into the bridge, Eqs. (4) and (5)

$$J = -(\kappa_{-1} + \kappa_1)A_0 + \kappa_1, \tag{A.4}$$

which results in the occupation probability on the first bridge unit

$$A_0 = \frac{\kappa_1 - k\alpha}{(\kappa_{-1} + \kappa_1)}. \tag{A.5}$$

From the two expressions for A_0, Eqs. (A.3) and (A.5), we obtain

$$\frac{\kappa_2 + k\alpha}{\kappa_2 + \kappa_{-2}} + N\alpha = \frac{\kappa_1 - k\alpha}{(\kappa_{-1} + \kappa_1)}. \tag{A.6}$$

Eq. (A.6) constitutes an equation for the unknown parameter α, whose solution is given by Eq. (11).

Appendix B. Steady state current for voltage biased hopping rates

Because of the steady state situation, the same current should enter the bridge from the electrode, where, according to Eq. (4),

$$J = \kappa_1 - (\kappa_1 + \kappa_{-1})A_0 \tag{B.1}$$

and the same current should leave the terminal bridge unit, where, according to Eq. (5)

$$J = \kappa_{-2}A_N - \kappa_2(1 - A_N) = (\kappa_2 + \kappa_{-2})A_N - \kappa_2. \tag{B.2}$$

Expressions for the steady state occupation probabilities inside the bridge were obtained in terms of the current J, Eq. (25), and the occupation, A_0, of the zeroth bridge unit, in the form

$$A_j = \left(k\gamma^{2j}A_0 - \frac{\gamma^{2j} - 1}{\gamma^2 - 1}J_{ss}\right)\frac{1}{k\gamma^{-1}}. \tag{B.3}$$

From the steady state condition on the occupation of the terminal bridge unit, Eq. (24), together with the expression for the occupation probability of the $(N-1)$th unit, one obtains A_N (expressed in terms of the two unknowns J and A_0) in the form

$$A_N = \frac{1}{(\gamma^{-1}k + \kappa_2 + \kappa_{-2})} \left[\kappa_2 + \left(k\gamma^{2(N-1)}A_0 - \frac{1 - \gamma^{2(N-1)}}{1 - \gamma^2}J \right)\gamma^2 \right].$$
(B.4)

The current out of the terminal unit is given by $(\kappa_2 + \kappa_{-2})A_N - \kappa_2$, which results in the equation

$$J\left[1 + \frac{(\kappa_2 + \kappa_{-2})}{(\gamma^{-1}k + \kappa_2 + \kappa_{-2})} \frac{1 - \gamma^{2(N-1)}}{1 - \gamma^2}\gamma^2 \right]$$
$$= \frac{(\kappa_2 + \kappa_{-2} - k\gamma^{2N})A_0}{(\gamma^{-1}k + \kappa_2 + \kappa_{-2})} - \frac{\gamma^{-1}k\kappa_2}{(\gamma^{-1}k + \kappa_2 + \kappa_{-2})}.$$
(B.5)

The occupation probability of the zeroth unit can be deduced from the expression for the current that enters the bridge, Eq. (4),

$$J = \kappa_1 - (\kappa_1 + \kappa_{-1})A_0,$$
(B.6)

which results in

$$A_0 = \frac{\kappa_1 - J}{(\kappa_1 + \kappa_{-1})}.$$
(B.7)

Substituting Eq. (B.7) in Eq. (B.5) results in an implicit equation for the current,

$$J = \frac{(\kappa_2 + \kappa_{-2})}{(\gamma^{-1}k + \kappa_2 + \kappa_{-2})}\left[k\gamma^{2N}\frac{\kappa_1 - J}{(\kappa_1 + \kappa_{-1})} - \frac{1 - \gamma^{2(N-1)}}{1 - \gamma^2}\gamma^2 J \right]$$
$$- \frac{\gamma^{-1}k\kappa_2}{(\gamma^{-1}k + \kappa_2 + \kappa_{-2})},$$
(B.8)

whose solution gives Eq. (27).

Appendix C. Incoherent transport in a bridge composed of a donor–acceptor pair

The kinetic equations for the D–A bridge between two metallic electrodes are given by

$$\frac{dD}{dt} = \kappa_1(1 - D) - (\kappa_{-1} + k^{CT})D + k_-^{CT}A,$$
$$\frac{dA}{dt} = -(\kappa_{-2} + k^{CT})A + k^{CT}D + \kappa_2(1 - A),$$
(C.1)

where D and A stand for the populations of the donor and the acceptor, respectively. Without a potential bias the system is in equilibrium and no current can exist. This fact is not obvious from the kinetic equations. Based on the kinetic equations, one can obtain three expressions for the steady state current

$$J = \kappa_1(1 - D) - \kappa_{-1}D,$$
$$J = k^{CT}D - k_-^{CT}A,$$
(C.2)
$$J = \kappa_{-2}A - \kappa_2(1 - A).$$

In order for the current to vanish at $\Phi = 0$, three conditions should be fulfilled:

$$D = \frac{\kappa_1}{\kappa_1 + \kappa_{-1}},$$
(C.3A)
$$A = \frac{\kappa_2}{\kappa_2 + \kappa_{-2}}$$
(C.3B)

and

$$\frac{A}{D} = k^{CT}/k_-^{CT}.$$
(C.4)

The conditions are not independent. The current vanishes only if the following relation between the rate constants is satisfied

$$\frac{k^{CT}}{k_-^{CT}} = \frac{1 + (\kappa_{-1}/\kappa_1)}{1 + (\kappa_{-2}/\kappa_2)}.$$
(C.5)

This is a relation between the inter-bridge rate constants and the rate constants for the charge exchange on the two electrodes (that are in equilibrium, with equal Fermi level). The exchange rate constant between the molecule and the electrodes depends on the energy gap between the molecular states and the Fermi level. The formation of a junction potential at the surfaces, due to partial charge shifts, establishes the equilibrium conditions. In the limit of $\Phi = 0$ the electrical current

$$j = ek^{CT}D - ek_-^{CT}A$$
(C.6)

is expected to vanish which, on the basis of Eq. (C.3), implies that

$$j = \frac{ek^{CT}\kappa_1}{\kappa_1 + \kappa_{-1}} - \frac{ek_-^{CT}\kappa_2}{\kappa_2 + \kappa_{-2}} = 0; \quad \Phi = 0.$$
(C.7)

For a finite voltage bias, the electrical current is given by Eq. (34).

References

[1] J. Jortner, M.A. Ratner (Eds.), Molecular Electronics, Blackwell Science, Oxford, 1997.
[2] J. Jortner, C.N.R. Rao (Eds.), Pure and applied chemistry, vol. 74, 2002, p. 1491.
[3] A. Nitzan, Ann. Rev. Phys. Chem. 52 (2001) 681.
[4] M.A. Reed, C. Zhou, C.J. Muller, T.P. Burgin, J.M. Tour, Science 278 (1997) 252.
[5] W.D. Tian, S. Datta, S.H. Hong, J. Reifenberger, J.I. Henderson, C.P. Kubiak, J. Chem. Phys. 109 (1998) 2874.
[6] V. Mujica, M. Kemp, A. Roitberg, M.A. Ratner, J. Chem. Phys. 104 (1996) 7296.
[7] V. Mujica, A. Nitzan, Y. Mao, W. Davis, M. Kemp, A. Roitberg, M.A. Ratner, Adv. Chem. Phys. 107 (1999) 403.
[8] M. Reed, Proc. IEEE 87 (1999) 652.
[9] H.B. Weber, J. Reichert, F. Weigend, R. Ochs, D. Beckmann, M. Mayor, R. Ahlrichs, H.V. Lohneysen, Chem. Phys. 283 (2002) 113.

[10] E.G. Petrov, V. May, P. Hanggi, Chem. Phys. 281 (2002) 211.
[11] E.G. Petrov, V. May, P. Hanggi, Chem. Phys. 296 (2004) 251.
[12] A. Nitzan, J. Phys. Chem. A 1 (2001) 223.
[13] A. Nitzan, Israel J. Chem. 42 (2002) 163.
[14] S.S. Isied, M.Y. Ogawa, J.F. Wishart, Chem. Rev. 92 (1992) 381.
[15] E.G. Petrov, Y.V. Schevchenko, V.I. Teslenko, V. May, J. Chem. Phys. 115 (2001) 7107.
[16] H.-W. Fink, C. Schöneberger, Nature 398 (1999) 407.
[17] P.J. De Pablo, F. Moreno-Herrero, J. Colchero, J. Gómez-Herrero, P. Herrero, A.M. Baró, P. Ordejón, J.M. Soler, E. Artacho, Phys. Rev. Lett. 85 (2000) 4992.
[18] D. Porath, A. Bezryadin, S. de Vries, C. Dekker, Nature 403 (2000) 635.
[19] A.J. Storm, J. van Noort, S. de Vries, C. Dekker, Appl. Phys. Lett. 79 (2001) 3881.
[20] A.Yu. Kasumov, M. Kociak, S. Geo'ron, B. Reulet, V.T. Volkov, D.V. Klinov, H. Bouchiat, Science 291 (2001) 280.
[21] K.-H. Yoo, D.H. Ha, J.-O. Lee, J.W. Park, H. Kim, J.J. Kim, H.-Y. Lee, T. Kawai, H.Y. Choi, Phys. Rev. Lett. 87 (2001) 198102.
[22] C. Gómez-Navarro, F. Moreno-Herrero, P.J. de Pablo, J. Colchero, J. Gómez-Herrero, A.M. Baró, Proc. Nat. Acad. Sci. USA 99 (2000) 8484.
[23] K. Shimotani, T. Shigematsu, C. Manabe, H. Watanabe, M. Shimizu, J. Chem. Phys. 118 (2003) 8016.
[24] J. Jortner, M. Bixon, T. Langenbacher, M.E. Michel-Beyerle, Proc. Natl. Acad. Sci. USA 95 (1998) 12759.
[25] M. Bixon, B. Giese, S. Wessely, T. Langenbacher, M.E. Michel-Beyerle, J. Jortner, Proc. Natl. Acad. Sci. USA 96 (1999) 11713.
[26] M. Bixon, J. Jortner, J. Phys. Chem. B 104 (2000) 3906.
[27] M. Bixon, J. Jortner, J. Phys. Chem. A 105 (2001) 10322.
[28] M. Bixon, J. Jortner, Chem. Phys. 281 (2002) 393.
[29] M. Bixon, J. Jortner, J. Am. Chem. Soc. 123 (2001) 12556.
[30] G.B. Schuster, Acc. Chem. Res. 33 (2000) 253.
[31] B. Giese, Acc. Chem. Res. 33 (2000) 631.
[32] M.E. Nuñez, D.B. Hall, J.K. Barton, Chem. Biol. 6 (1999) 85.
[33] T.T. Williams, D.T. Odon, J.K. Barton, J. Am. Chem. Soc. 122 (2000) 9048.
[34] F.D. Lewis, X. Liu, J. Liu, S.E. Miller, R.T. Hayes, M.R. Wasielewski, Nature 406 (2000) 51.
[35] F.D. Lewis, X. Liu, J. Liu, R.T. Hayes, M.R. Wasielewski, J. Am. Chem. Soc. 122 (2000) 12037.
[36] F.D. Lewis, R.S. Kalgutkar, Y. Wu, X. Liu, J. Liu, R.T. Hayes, S.E. Miller, M.R. Wasielewski, J. Am. Chem. Soc. 122 (2000) 12346.
[37] E. Megger, M.E. Michel-Beyerle, B. Giese, J. Am. Chem. Soc. 120 (1998) 12950.
[38] B. Giese, S. Wessely, M. Spormann, U. Lindemann, E. Meggers, M.E. Michel-Beyerle, Angew. Chem. Int. Ed. 38 (1999) 996.
[39] B. Giese, S. Wessely, Angew. Chem. Int. Ed. 39 (2000) 3490.
[40] P.T. Henderson, D. Jones, G. Hampkian, Y. Kan, G.B. Schuster, Proc. Natl. Acad. Sci. USA 96 (1999) 8353.
[41] L. Sanii, G.B. Schuster, J. Am. Chem. Soc. 122 (2000) 11545.
[42] B. Giese, M. Spichty, Chem. Phys. Chem. 1 (2000) 195.
[43] B. Giese, J. Amaudrut, A.K. Kohler, M. Spermann, S. Wessely, Nature 412 (2001) 318.
[44] D. Segal, A. Nitzan, W.B. Davis, M.R. Wasielewski, M.A. Ratner, J. Phys. Chem. B 104 (2000) 3817.
[45] G. Brunaud, F. Castet, A. Fritsch, M. Kreissler, L. Ducasse, J. Phys. Chem. B 105 (2001) 12665.
[46] A. Troisi, G. Orlandi, Chem. Phys. Lett. 344 (2001) 509.
[47] F. Bogar, J. Ladik, Chem. Phys. 237 (1998) 273.
[48] L. Shen, Y.-J. Ye, J. Ladik, Solid State Commun. 121 (2002) 35.
[49] A.A. Voityuk, J. Jortner, M. Bixon, N. Rösch, Chem. Phys. Lett. 324 (2000) 427.
[50] A.A. Voityuk, N. Rösch, M. Bixon, J. Jortner, J. Phys. Chem. B 104 (2000) 9740.
[51] A.A. Voityuk, J. Jortner, M. Bixon, N. Rösch, J. Chem. Phys. 114 (2001) 5614.
[52] F. Gutman, L.E. Lyons, Organic Semiconductors, John Wiley, New York, 1966.
[53] R.J.O.M. Hoofman, M.P. de Haas, L.D.A. Siebbeles, J.M. Warman, Nature 392 (1998) 54.
[54] F.C. Gorzema, L.D.A. Siebbeles, J.M. Warman, S. Seki, S. Tagawa, U. Scharf, Adv. Mater. 14 (2002) 228.
[55] M. Bixon, J. Jortner, Adv. Chem. Phys. 107 (1999) 35.
[56] F.C. Grozema, P.Th. van Duijnen, Y.A. Berlin, M.A. Ratner, L.D.A. Siebbeles, J. Phys. Chem. B 106 (2002) 7791.
[57] M. Bixon, J. Jortner, to be published.